NJC

PAPER

View Article Online
View Journal

Cite this: DOI: 10.1039/c8nj00685g

Enantiomeric separation and simulation study of eight anticholinergic drugs on an immobilized polysaccharide-based chiral stationary phase by HPLC

Meng Li,[a] Bo Zhang,[a] Jia Yu,[a] Jian Wang*[b] and Xingjie Guo *[a]

Received 8th February 2018,
Accepted 4th June 2018

DOI: 10.1039/c8nj00685g

rsc.li/njc

The enantiomeric separation of eight anticholinergic drugs was first systematically examined on a derivative polysaccharide chiral stationary phase (CSP), *i.e.* Chiralpak ID in the normal phase mode. Except for scopolamine hydrobromide and benzhexol hydrochloride, the other six analytes including atropine sulfate, phencynonate, dipivefrine hydrochloride, tropicamide, homatropine methylbromide and oxybutynin were either completely or partially separated under the optimized mobile phase conditions with resolutions of 3.98, 2.52, 2.02, 2.14, 1.80 and 0.41, respectively. The influences of organic modifier types and content, and base/acid additives on enantiomeric separation were evaluated and optimized. Furthermore, a simulation study was also used to explain the chiral recognition mechanisms of this class of drug enantiomers on Chiralpak ID for the first time. The modeling data were in agreement with the chromatographic results concerning enantioselectivity.

1. Introduction

The enantiomeric separation of chiral drugs has become increasingly important due to the different pharmacodynamic and/or pharmacokinetic properties of the two enantiomers.[1–4] The diverse stereoselectivity of an individual enantiomer *in vivo* might cause a range of side effects to the human body. Hence, in order to improve the safety of clinical medication and provide convenient research into the biological properties of each enantiomer, the development of chiral analytical methods is an urgent need within the pharmaceutical industry.

Up until now high performance liquid chromatography (HPLC) using chiral stationary phases (CSPs) was considered as the best technique for analysis and separation of drug enantiomers. Among the CSPs employed in HPLC, polysaccharide-based CSPs, especially amylose derivatives, as chiral selectors were the most successful in terms of enantiomeric separation. They possessed advantages in CSPs such as robustness and exhibited a wide range of applications.[5–7] However, the chiral recognition mechanisms of these CSPs were not yet completely elucidated.[8]

Anticholinergic drugs, usually known as the cholinoceptor antagonists, are mainly used in clinics for spasmolysis, mydriasis and dilated bronchi.[9] Most of this class of drug, like atropine, have been commonly formulated and administered as racemates. As the previous article reported, it was confirmed that the two enantiomers of atropine possess different pharmacological activities.[10] Additionally, it was found that the (+)- and (−)-isomers of benzhexol differed in the affinity of acetylcholine receptors.[11] Therefore, keeping in mind these facts, the enantiomeric separation of this class of drug enantiomers was very important and necessary.

At present there are only a few papers that have studied the enantiomeric separation of some anticholinergic drugs by capillary electrophoresis (CE) and HPLC.[12–16] Therein, atropine and benzhexol were completely separated with different β-cyclodextrin derivatives as chiral additives by CE. Furthermore, the enantiomers of oxybutynin were baseline resolved on two coated amylose-based columns (AmyCoat and Chiralpak AD) with *n*-hexane–2-propanol–DEA (80 : 20 : 0.1, v/v) as the mobile phase. Beyond that, however, almost no paper has been concerned with the enantiomeric separation of the anticholinergic drugs using immobilized amylose-based CSPs.

In recent years, in order to determine the chiral recognition mechanisms of the CSPs at the molecular level, several computational simulations focusing on the enantiomeric separation, particularly by molecular docking, have been developed.[17–21] The modeling technique could gain better insight into the binding energy between each enantiomer and the CSP, and clarify the types of intermolecular interactions. Therefore, it was efficient and accurate to explain the chiral recognition process. For instance, I. Ali *et al.*[16] applied simulation studies to investigate the enantioseparation of four chiral analytes on the AmyCoat chiral selector. The significant difference in the binding affinity and

[a] School of Pharmacy, Shenyang Pharmaceutical University, Shenyang, Liaoning Province, 110016, P. R. China. E-mail: gxjhyz@gmail.com
[b] School of Pharmaceutical Engineering, Shenyang Pharmaceutical University, Shenyang, Liaoning Province, 110016, P. R. China. E-mail: jianwang@syphu.edu.cn

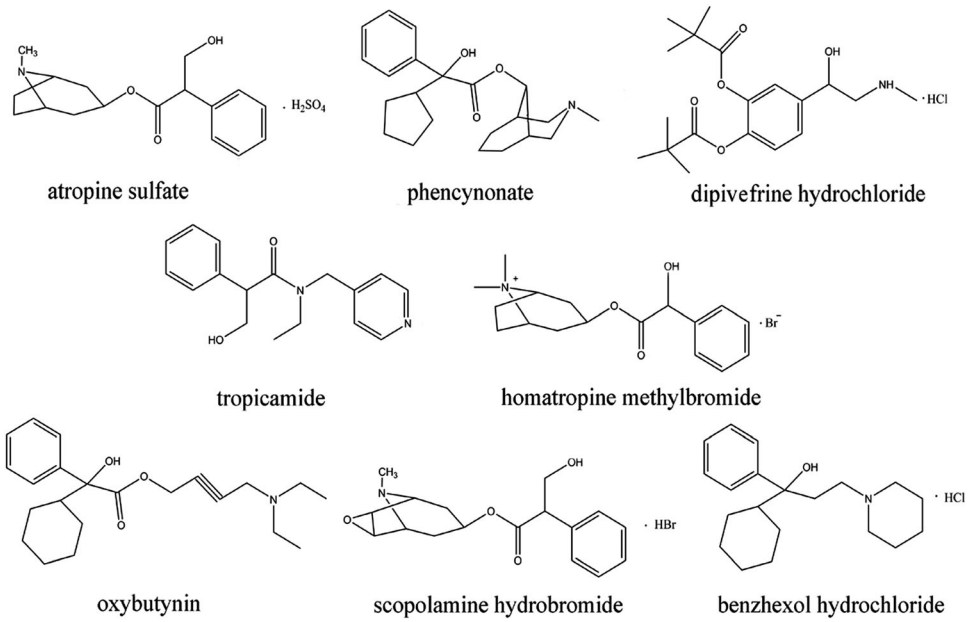

Fig. 1 The chemical structures of eight analytes.

the specific interactions for separation were found. M. F. Alajmi *et al.*[22] studied the separation mechanisms of DL-leucine-DL-tryptophan dipeptide on a tris-(3,5-dimethylphenyl carbamate) amylose chiral selector using a modeling method. However, a thorough search of the literature confirmed that a simulation study for the chiral separation of anticholinergic drugs with immobilized amylose-based CSPs has not been reported until now.

Herein, we explored for the first time an efficient HPLC analytical method for the enantiomeric separation of eight analytes including atropine sulfate, phencynonate, dipivefrine hydrochloride, tropicamide, homatropine methylbromide, oxybutynin, scopolamine hydrobromide and benzhexol hydrochloride (Fig. 1). The tested column was Chiralpak ID (Fig. 2), which was a commercially immobilized polysaccharide-based CSP, namely, amylose tris-(3-chlorophenylcarbamate). In addition, the influences of alcohol-modifying agents and basic/acidic additives on enantiomeric separation were evaluated and optimized in detail. Furthermore, molecular docking using AutoDock was carried out to ascertain the possible chiral recognition mechanisms of Chiralpak ID for the first time. The results of these experiments are given herein.

2. Experimental

2.1 Chemicals and reagents

The standard substances of atropine sulfate, phencynonate, dipivefrine hydrochloride, tropicamide, homatropine methylbromide, oxybutynin, scopolamine hydrobromide and benzhexol hydrochloride were obtained from the Chinese Food and Drug Inspection Institute (Beijing, China). HPLC grade *n*-hexane, ethanol, 2-propanol and 1-propanol were purchased from Concord Technology (Tianjin, China). Formic acid (FA) and diethylamine (DEA) were of analytical grade and supplied from Shandong Yuwang Industrial (Shandong, China).

2.2 Chromatographic conditions

The experiments were performed on a Shimadzu LC-10A HPLC system (Shimadzu, Japan) equipped with an LC-10AT pump and an SPD-10A UV-vis Detector. The detection signals and data were collected and processed by the Sepu3000 software (Hangzhou, China). The stationary phase was the commercially available Chiralpak ID (250 mm × 4.6 mm, 5 μm) column purchased from Daicel Chiral Technologies (Shanghai, China). The mobile phase systems consisted of *n*-hexane–ethanol/2-propanol/1-propanol. The prepared mobile phase was filtered and de-gassed before use. The column was maintained at 25 °C, and the injection volume was 20 μL. The flow rate was 1.0 mL min^{-1} and the detection wavelength was set at 230 nm.

2.3 Preparation of sample solutions

All eight analytes studied were dissolved in ethanol to prepare stock solutions of 1 mg mL^{-1}, and were then diluted to a suitable concentration, respectively. All solutions were filtered through an organic nylon membrane of 0.45 μm pore size.

2.4 Calculations

The chromatographic parameters of retention factor (k), separation factor (α) and resolution (Rs) were calculated as follows: $k = (t_R - t_0)/t_0$, where t_R and t_0 represented the retention times of the analytes and the unretained solutes, respectively; $\alpha = k_2/k_1$, where k_1 and k_2 were the retention factors of the first and second eluted enantiomers; $Rs = 2(t_2 - t_1)/(W_1 + W_2)$, where t_1 and t_2 were the retention times of the successively eluted enantiomers, and W_1 and W_2 were the peak widths of the first and second eluted enantiomers, respectively.

2.5 Simulation study

The system of Intel® Xeon E5-2670 with Red hat 6.4 was used for molecular docking of the eight drug enantiomers. The Marwin

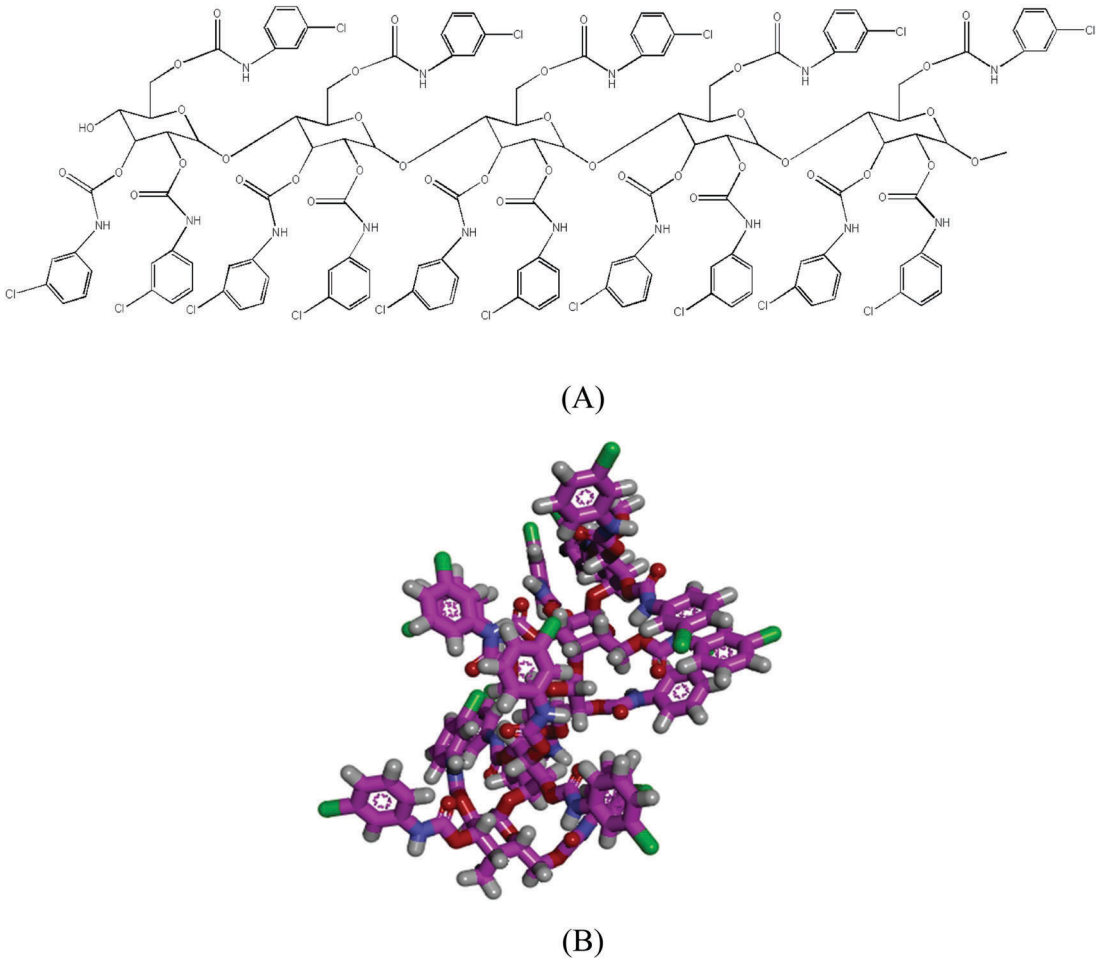

Fig. 2 The 2D (A) and 3D (B) structures of the amylose tris-(3-chlorophenylcarbamate) chiral selector (Chiralpak ID).

Sketch software was used to draw the structures of the studied enantiomers and Chiralpak ID. The structures were transferred to 3D and saved in mol2 file format. Sybyl 6.9.1 based on the molecular mechanics minimization was used to optimize the structures. After that, using AutoDock 4.2, the enantiomers and the CSP were prepared by assigning Gastegier charges, merging nonpolar hydrogen atoms and saving in PDBQT file format. The automated molecular docking was done with AutoDock 4.2, and the grid box size of 120 × 120 × 120 points with 0.75 Å spacing was applied. One hundred independent docking runs were used for each enantiomer and the CSP for the lowest free energy of the fastening conformation from the largest cluster, which was saved in PDBQT file format. Finally, Discovery Studio Visualizer was used for molecular display.

3. Results and discussion

3.1 Chromatographic separation of eight drug enantiomers

As a general rule, Chiralpak ID is mainly used to resolve drug enantiomers under normal phase mode. Thus, the enantiomeric separation of eight analytes was evaluated with the alcohol-modifying agents ethanol, 2-propanol and 1-propanol. In our previous study, only tropicamide was baseline resolved under the *n*-hexane–alcohol systems without the addition of DEA or DEA and FA. As the eight analytes were basic, a small amount of base (0.1% DEA) was added to the mobile phase to reduce the peak tail and to obtain a good peak shape. The results revealed that the enantiomeric separation of some analytes, such as atropine sulfate, homatropine methylbromide and tropicamide, was significantly improved. To optimize further the chiral HPLC conditions, a mixture of 0.1% DEA and 0.1% FA was used to study the chiral separation of the eight analytes. It was shown that a total of four analytes including atropine sulfate, phencynonate, dipivefrine hydrochloride and tropicamide were completely separated with an Rs larger than 1.5, and one analyte, *i.e.* oxybutynin, was partially separated. However, it was interesting to note that the enantioselectivity of homatropine methylbromide was not observed, indicating that different acidic and basic additives might result in different chiral separation.

To some extent, the ability of the enantiomeric separation of 2-propanol and 1-propanol was better than that of ethanol. Nevertheless, the exception was atropine sulfate which achieved the largest resolution using ethanol as the alcohol modifier. From Table 1, we concluded that five of the eight analytes were baseline resolved, one was partially separated and two were not

Table 1 Enantiomeric separation of the six analytes on Chiralpak ID under optimized conditions

Analytes	k_1	α	Rs	Mobile phase
Atropine sulfate	2.82	1.35	3.98	*n*-Hexane–ethanol–DEA–FA (60 : 40 : 0.1 : 0.1, v/v/v/v)
Phencynonate	1.75	1.21	2.52	*n*-Hexane–2-propanol–DEA–FA (75 : 25 : 0.1 : 0.1, v/v/v/v)
Dipivefrine hydrochloride	2.48	1.20	2.02	*n*-Hexane–2-propanol–DEA–FA (75 : 25 : 0.1 : 0.1, v/v/v/v)
Tropicamide	1.59	1.15	2.14	*n*-Hexane–ethanol–DEA–FA (60 : 40 : 0.1 : 0.1, v/v/v/v)
Homatropine methylbromide	0.95	1.14	1.80	*n*-Hexane–1-propanol–DEA (85 : 15 : 0.1, v/v/v)
Oxybutynin	1.59	1.10	0.41	*n*-Hexane–2-propanol–DEA–FA (80 : 20 : 0.1 : 0.1, v/v/v/v)

Flow rate: 1.0 mL min^{-1}; column temperature: 25 °C; detection wavelength: 230 nm; injection volume: 20 μL.

separated under the optimized chromatographic conditions. The k_1 values of atropine sulfate, phencynonate, dipivefrine hydrochloride, tropicamide, homatropine methylbromide and oxybutynin were 2.82, 1.75, 2.48, 1.59, 0.95 and 1.59, respectively. The values of α and Rs were 1.35, 1.21, 1.20, 1.15, 1.14 and 1.10, and 3.98, 2.52, 2.02, 2.14, 1.80 and 0.41, respectively. The chiral separation of the above six analytes was acceptable because the magnitudes of α and Rs were larger than 1.0 and 1.5, respectively.

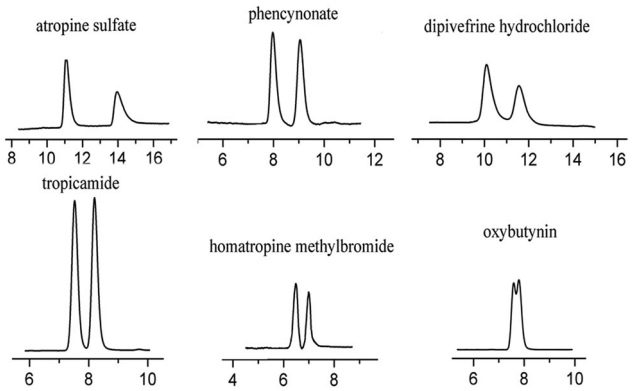

Fig. 3 Typical chromatograms of chiral separation of atropine sulfate, phencynonate, dipivefrine hydrochloride, tropicamide, homatropine methylbromide and oxybutynin on Chiralpak ID under the optimal chromatographic conditions.

On the basis of the above studies, we selected the optimal mobile phase composition of each analyte to study the effect of alcohol content on enantioseparation. For the six separated drugs, we found that the k and Rs values increased with a decrease in alcohol content in the mobile phase, indicating that the chiral separation was strongly influenced by the polarity of the mobile phase. However, the α value remained basically unchanged.

The flow rate, which varied from 0.6 to 1.0 mL min^{-1}, was also evaluated and it was observed that a decrease in the flow rate resulted in a prolonged retention time and better separation. However, the longer analysis times could result in a larger occurrence rate of wide peaks and low column efficiency. Thereby, 1.0 mL min^{-1} was chosen as the best flow rate. Moreover, the column temperature (25–40 °C) was investigated to optimize the chromatographic conditions. The conclusion was that a higher column temperature harmed the chiral separation of the studied analytes.

As a result of the experiments, optimized enantiomeric separation conditions of eight drug enantiomers were confirmed and reported (Table 1), and the corresponding chromatograms are shown in Fig. 3.

3.2 Simulation study of eight drug enantiomers with Chiralpak ID

Molecular docking of atropine sulfate, phencynonate, dipivefrine hydrochloride, tropicamide, homatropine methylbromide, oxybutynin, scopolamine hydrobromide and benzhexol hydrochloride

Table 2 The modeling results of the enantiomers of the eight studied analytes with Chiralpak ID

Analytes	Enantiomers	Binding affinity/energy (kcal mol^{-1})	Number of hydrogen bonds	Number of hydrophobic interactions	ΔE_{R-S}[a]
Atropine sulfate	*R*	−7.68	2	1	−0.58
	S	−7.10	1	2	
Phencynonate	*R*	−7.47	2	1	0.26
	S	−7.73	1	4	
Dipivefrine hydrochloride	*R*	−6.71	6	2	0.22
	S	−6.93	3	3	
Tropicamide	*R*	−6.49	2	2	0.24
	S	−6.73	2	5	
Homatropine methylbromide	*R*	−6.92	2	2	0.13
	S	−7.05	5	1	
Oxybutynin	*R*	−6.76	2	2	0.05
	S	−6.81	2	1	
Scopolamine hydrobromide	*R*	−6.42	1	2	−0.03
	S	−6.39	3	2	
Benzhexol hydrochloride	*R*	−7.73	0	2	−0.01
	S	−7.72	0	6	

[a] Difference in the binding energies of enantiomers.

with amylose tris-(3-chlorophenylcarbamate) (Chiralpak ID) was carried out to investigate the chiral recognition mechanisms. The modeling results are outlined below in detail.

3.2.1 Molecular docking calculations. The binding energies for the best scoring, *i.e.* the lowest binding affinity, conformation of the (*R*)- and (*S*)-enantiomers with CSP are shown in Table 2. The different values of the binding energies of the drug enantiomers with CSP depended on the various stereochemical structures of the drugs, which were maintained by different types and numbers of intermolecular interaction forces. Meanwhile, the results also implied that the stability of the enantiomer in combination with CSP was different. The more negative the binding energy, the stronger the interaction was that was established between the enantiomers and CSP.[23]

In order to further elaborate on the relationship between the enantiomeric separation and the binding energy, the difference in the binding energies of the (*R*)- and (*S*)-enantiomers with CSP (ΔE_{R-S}) was calculated. If the absolute value of ΔE_{R-S} was larger, it would contribute more to the difference in retention time of the two enantiomers. Thus, the enantiomeric separation might be easier to achieve. From Table 2 it could be seen that the ΔE_{R-S} values of the eight analytes mentioned above were −0.58, 0.26, 0.22, 0.24, 0.13, 0.05, −0.03 and −0.01 kcal mol^{-1}, respectively. Among them, the atropine sulfate enantiomers showed the biggest energy difference (ΔE_{R-S} = −0.58 kcal mol^{-1}), whereas the ΔE_{R-S} values of the scopolamine hydrobromide (−0.03 kcal mol^{-1}) and benzhexol hydrochloride (−0.01 kcal mol^{-1}) enantiomers were much smaller than those of any other analytes. Therefore, it was hypothesized that atropine would have the larger resolution. On the other hand, the smaller resolution would be acquired for the scopolamine hydrobromide and benzhexol hydrochloride. According to the previous enantiomeric separation

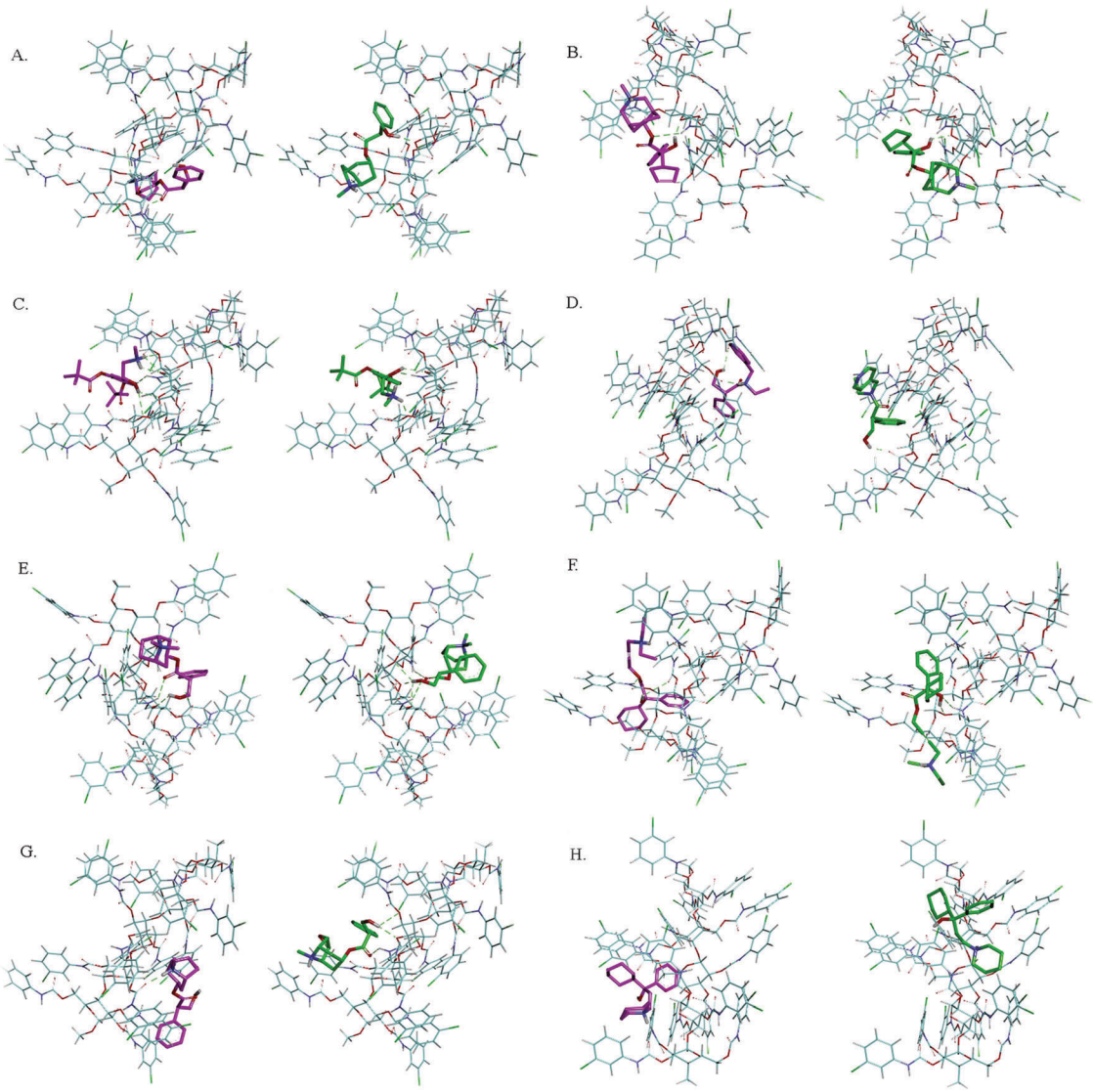

Fig. 4 The 3D docking positions of the two enantiomers of the studied analytes with CSP: (A) atropine sulfate, (B) phencynonate, (C) dipivefrine hydrochloride, (D) tropicamide, (E) homatropine methylbromide, (F) oxybutynin, (G) scopolamine hydrobromide and (H) benzhexol hydrochloride. Purple represents the (*R*)-enantiomer of the analytes, green represents the (*S*)-enantiomer and the green dotted lines represent the hydrogen bonds.

results, atropine sulfate was completely separated with the largest Rs of 3.98 and no chiral separation for scopolamine hydrobromide and benzhexol hydrochloride was found on Chiralpak ID. These results were consistent with our expectation.

3.2.2 The hydrogen bond interaction. The three-dimensional docking conformations of the eight drug enantiomers interacting with CSP are shown in Fig. 4. It is clear that the drug enantiomers are stable at different positions in the chiral grooves of CSP through hydrogen bonds and other interactions. From Table 3 and Fig. 4, it can be seen that the structures of carbonyl (C═O), hydroxyl (–OH) and amino groups near the chiral carbon atom of the drug enantiomers could form stronger hydrogen bonds with the amino, C═O and ether (–O–) groups of CSP. These interactions were found between the polar atoms and were called conventional hydrogen bonds.

For the eight chiral drugs, the type and number of hydrogen bonds were significantly different due to the difference in the stereochemical structure of the drug enantiomers. For example, the C═O and –OH groups of three structurally similar analytes including atropine sulfate, homatropine methylbromide and scopolamine hydrobromide formed hydrogen bonds with the amino and –O– groups of CSP, respectively. However, the number and type of hydrogen bonds between the (*R*)- or (*S*)-enantiomers and CSP were clearly different. Taking atropine sulfate and scopolamine hydrobromide as examples, it was found that for (*R*)- and (*S*)-atropine sulfate, two and one hydrogen bonds were formed between the oxygen of the C═O group in atropine and the hydrogen of the –NH– group in CSP and the hydrogen of the amino group in atropine and the oxygen of the C═O group in CSP, and the hydrogen of the –OH group of atropine and the oxygen of the –O– group in CSP, respectively. For scopolamine hydrobromide, a hydrogen bond for the (*R*)-enantiomer was generated by the hydrogen of the amine group in scopolamine and the oxygen of the C═O group in CSP, while for the (*S*)-enantiomer, the hydrogen of the –OH group in scopolamine and the oxygen atoms of two different –O– groups in CSP and the oxygen of the C═O group in scopolamine and hydrogen of the –NH group in CSP formed three hydrogen bonds. Additionally, the C═O groups in the oxybutynin, phencynonate and dipivefrine hydrochloride molecules did not form hydrogen bonds with CSP. We inferred that the larger or longer side chains near the carbonyl might affect the access to the chiral grooves of CSP, resulting in a greater distance to the amine groups of the CSP (Fig. 4). For benzhexol hydrochloride, a hydrogen bond was not found and its enantiomeric separation was not obtained at the same time. These results were enough to show that the hydrogen bond played an important role in chiral separation of this set of drug enantiomers.

3.2.3 The hydrophobic interaction. The hydrophobic interaction can also be observed from Table 4. Three kinds of hydrophobic interaction including pi hydrophobic, alkyl hydrophobic and mixed pi–alkyl hydrophobic were observed and were present in different enantiomers of the studied analytes and CSP. It can be seen that the distance of all hydrophobic interactions was larger than 3.65 Å, indicating that the hydrophobic interaction of the enantiomers and CSP was weaker to

Table 3 The hydrogen bonds of the studied analytes with CSP

Analyte	Enantiomer	Name	Type	Distance (Å)
Atropine sulfate	*R*	:⟨1⟩:H319–d:RES1:O4, d:RES1:H42–:⟨1⟩:O165[a]	Conventional hydrogen bond	1.61, 2.49
	S	d:RES1:H32–:⟨1⟩:O103	Conventional hydrogen bond	1.91
Phencynonate	*R*	:⟨1⟩:H267–d:RES1:O14, d:RES1:H58–:⟨1⟩:O103	Conventional hydrogen bond	2.85, 1.80
	S	d:RES1:H58–:⟨1⟩:O90	Conventional hydrogen bond	2.03
Dipivefrine hydrochloride	*R*	:⟨1⟩:H267–d:RES1:O3, d:RES1:H30–:⟨1⟩:O103, d:RES1:H31–:⟨1⟩:O103, d:RES1:H31–:⟨1⟩:O114, d:RES1:H29–:⟨1⟩:O90, d:RES1:H29–:⟨1⟩:O125	Conventional hydrogen bond	2.55, 2.03, 2.19, 2.17, 2.14, 2.59
	S	:⟨1⟩:H267–d:RES1:O3, d:RES1:H30–:⟨1⟩:O125, d:RES1:H29–:⟨1⟩:O103	Conventional hydrogen bond	1.95, 1.97, 2.15
Tropicamide	*R*	d:RES1:H26–:⟨1⟩:O72, d:RES1:H22–:⟨1⟩:O42	Conventional hydrogen bond	1.94, 2.42
	S	:⟨1⟩:H267–d:RES1:O21, d:RES1:H41–:⟨1⟩:O154	Conventional hydrogen bond	2.21, 1.92
Homatropine methylbromide	*R*	:⟨1⟩:H267–d:RES1:O19, d:RES1:H42–:⟨1⟩:O103	Conventional hydrogen bond	2.68, 2.17
	S	:⟨1⟩:H267–d:RES1:O20, :⟨1⟩:H294–d:RES1:O19, d:RES1:H42–:⟨1⟩:O90, d:RES1:H42–:⟨1⟩:O103, d:RES1:H42–:⟨1⟩:O125	Conventional hydrogen bond	2.65, 3.09, 1.94, 2.48, 2.56
Oxybutynin	*R*	:⟨1⟩:H289–d:RES1:O11, d:RES1:H38–:⟨1⟩:O165	Conventional hydrogen bond	1.78, 2.86
	S	:⟨1⟩:H267–d:RES1:O9, d:RES1:H38–:⟨1⟩:O125	Conventional hydrogen bond	2.47, 2.13
Scopolamine hydrobromide	*R*	d:RES1:H41–:⟨1⟩:O137	Conventional hydrogen bond	1.85
	S	:⟨1⟩:H267–d:RES1:O4, d:RES1:H33–:⟨1⟩:O103, d:RES1:H33–:⟨1⟩:O114	Conventional hydrogen bond	2.37, 2.10, 2.91
Benzhexol hydrochloride	*R*	—	—	—
	S	—	—	—

[a] d:RES1 represents the drug enantiomers, and :⟨1⟩ represents CSP.

Table 4 The hydrophobic interaction of the studied analytes with CSP

Analytes	Enantiomers	Name	Types	Distance (Å)
Atropine sulfate	*R*	d:RES1–:⟨1⟩:Cl71[a]	Pi–alkyl	5.07
	S	d:RES1–:⟨1⟩:Cl29, d:RES1–:⟨1⟩:Cl61	Pi–alkyl, pi–alkyl	4.14, 5.32
Phencynonate	*R*	d:RES1–:⟨1⟩:Cl29	Pi–alkyl	4.38
	S	:⟨1⟩:Cl112–d:RES1, :⟨1⟩–d:RES1, d:RES1–:⟨1⟩:Cl29, d:RES1–:⟨1⟩:Cl61	Alkyl, pi–alkyl, pi–alkyl, pi–alkyl	5.14, 4.98, 4.04, 5.19
Dipivefrine hydrochloride	*R*	d:RES1:C17–:⟨1⟩, d:RES1–:⟨1⟩:Cl29	Pi–sigma, pi–alkyl	3.65, 4.46
	S	d:RES1:C16–:⟨1⟩, :⟨1⟩–d:RES1, d:RES1–:⟨1⟩:Cl29	Pi–sigma, pi–pi T-shaped, pi–alkyl	3.74, 5.96, 5.19
Tropicamide	*R*	d:RES1–:⟨1⟩:Cl164, d:RES1–:⟨1⟩	Pi–alkyl, pi–alkyl	4.20, 5.42
	S	d:RES1:C18–:⟨1⟩, :⟨1⟩–d:RES1, :⟨1⟩–d:RES1, d:RES1–:⟨1⟩:Cl29, d:RES1–:⟨1⟩:Cl61	Pi–sigma, pi–pi stacked, pi–pi T-shaped, pi–alkyl, pi–alkyl	3.90, 4.57, 5.81, 4.45, 5.19
Homatropine methylbromide	*R*	d:RES1–:⟨1⟩:Cl29, d:RES1–:⟨1⟩:Cl61	Pi–alkyl, pi–alkyl	4.30, 5.22
	S	d:RES1–:⟨1⟩:Cl61	Pi–alkyl	4.65
Oxybutynin	*R*	d:RES1–:⟨1⟩:Cl71, d:RES1–:⟨1⟩:Cl102	Pi–alkyl, pi–alkyl	4.40, 4.72
	S	d:RES1–:⟨1⟩:Cl29	Pi–alkyl	4.76
Scopolamine hydrobromide	*R*	:⟨1⟩–d:RES1, d:RES1–:⟨1⟩:Cl206	Pi–pi stacked, pi–alkyl	3.88, 4.41
	S	d:RES1–:⟨1⟩:Cl29, d:RES1–:⟨1⟩:Cl61	Pi–alkyl, pi–alkyl	4.44, 5.36
Benzhexol hydrochloride	*R*	:⟨1⟩:Cl29–d:RES1, :⟨1⟩–d:RES1:C8	Alkyl, pi–alkyl	4.73, 4.73
	S	:⟨1⟩:Cl19–d:RES1:C8, :⟨1⟩–d:RES1:C8, :⟨1⟩–d:RES1:C8, :⟨1⟩–d:RES1:C8, :⟨1⟩–d:RES1, d:RES1–:⟨1⟩:Cl71	Alkyl, pi–alkyl, pi–alkyl, pi–alkyl, pi–alkyl, pi–alkyl	4.05, 4.26, 5.29, 5.10, 5.09, 4.85

[a] d:RES1 represents the drug enantiomers, and :⟨1⟩ represents CSP.

some extent. The type and number of hydrophobic interactions were related to the structure of the drug enantiomers. The pi–alkyl interactions of atropine sulfate, homatropine methylbromide, scopolamine hydrobromide and tropicamide were mainly formed by the enantiomers with Pi orbitals and CSP with Cl atoms. Interestingly, for (*R*)- and (*S*)-tropicamide, the pyridine ring in the molecule generated additional pi–alkyl and pi–pi hydrophobic interactions with CSP, respectively. A number of different pi–alkyl interactions were developed between the structures of cyclopentane in the phencynonate molecule and the piperidine ring in the benzhexol hydrochloride molecule with the phenyl moiety of CSP, respectively. Moreover, due to the presence of methyl in dipivefrine hydrochloride, a pi–sigma hydrophobic interaction was found.

From the modeling results, except for the stronger hydrogen bond interaction, it was important to note that the hydrophobic interaction was also key for the chiral separation. A large amount of pi–alkyl (–Cl) hydrophobic interactions between the enantiomers and CSP clearly demonstrated that the substituents on the benzene ring of CSP were crucial for enantiomeric separation. Therefore, in light of these facts, we have sufficient reason to think that the interactions mentioned above make a significant contribution to the enantiomeric separation of the studied analytes.

4. Conclusion

In this paper, the enantiomeric separation of eight anticholinergic drugs on a polysaccharide-based CSP was first investigated in normal phase mode. The conditions of enantiomeric separation were evaluated and optimized by changing the mobile phase as well as the base and acid additives. Under the optimized conditions, five out of eight of the drug enantiomers were baseline resolved, and one was partially separated. Additionally, a simulation study was first used to illustrate the chiral recognition mechanisms, and the docking results were in accordance with the chromatographic parameters regarding enantioselectivity. The hydrogen bonds and hydrophobic interactions played a crucial role for the enantiomeric separation.

Conflicts of interest

There are no conflicts to declare.

References

1 J. W. Oh, T. Q. Trung, K. S. Sin, J. S. Kang and K. H. Kim, *Chirality*, 2007, **19**, 528–535.
2 S. Yuan and Q. L. Zeng, *Chromatographia*, 2017, **80**, 1171–1177.
3 F. Jamali, R. Mehvar and F. M. Pasutto, *J. Sep. Sci.*, 1989, **78**(9), 695–715.
4 C. Alvarez, J. A. Sanchez-Brunete, S. Torrado-Santiago, R. Cadorniga and J. J. Torrado, *Chromatographia*, 2000, **52**(7–8), 455–458.
5 E. Yashima, *J. Chromatogr. A*, 2001, **906**, 105–125.
6 S. Materazzo, S. Carradori, R. Ferretti, B. Gallinella, D. Secci and R. Cirilli, *J. Chromatogr. A*, 2014, **1327**, 73–79.
7 R. Geryk, K. Kalíková, J. Vozka, D. Plecitá, M. G. Schmid and E. Tesarová, *J. Chromatogr. A*, 2014, **1363**, 155–161.
8 R. W. Stringham, *Adv. Chromatogr.*, 2007, **38**, 257–290.

9 Q. D. You, Chem. Ind. Press, 2008.
10 L. Mateus, S. Cherkaoui, P. Christen and J. L. Veuthey, *J. Chromatogr. A*, 2000, **868**, 285–294.
11 R. B. Barlow, *J. Pharm. Pharmacol.*, 1971, **23**(2), 90–97.
12 G. H. Du, S. Y. Lu, L. H. Liu, J. W. Xie, B. H. Zhong and K. L. Liu, *Chin. J. Pharm. Anal.*, 2007, **27**(9), 1395–1398.
13 X. L. Lin, G. B. Li, W. Q. Jiang, Y. B. Chu, P. Wu and Y. F. Guan, *Anal. Chim. Acta*, 2001, **431**, 41–48.
14 M. M. Hefnawy and J. T. Stewart, *Anal. Lett.*, 1998, **31**(4), 659–667.
15 S. I. Tahara, A. Okayama, Y. Kitada, T. Watanabe, H. Nakazawa, K. Kakehi and Y. Hisamatu, *J. Chromatogr. A*, 1999, **848**, 465–471.
16 I. Ali, Z. A. Al-Othman, A. Al-Warthan, S. D. Alam and J. A. Farooqi, *Chirality*, 2014, **26**, 136–143.
17 W. H. Li, C. H. Liu, G. G. Tan, X. R. Zhang, Z. Y. Zhu and Y. F. Chai, *Int. J. Mol. Sci.*, 2012, **13**, 710–725.
18 C. Fernandes, M. E. Tiritan, Q. Cass, V. Kairys, M. X. Fernandes and M. Pinto, *J. Chromatogr. A*, 2012, **1241**, 60–68.
19 I. Ali, M. N. Lone, M. Suhail, Z. A. AL-Othmanb and A. Alwarthan, *RSC Adv.*, 2016, **6**(17), 14372–14380.
20 C. Fernandes, A. Palmeira, A. Santos, M. E. Tiritan, C. Afonso and M. M. Pinto, *Chirality*, 2013, **25**, 89–100.
21 H. Y. Aboul-Enein, I. Ali, M. Laguerre and G. Felix, *J. Liq. Chromatogr. Relat. Technol.*, 2002, **25**, 2739–2748.
22 M. F. Alajmi, A. Hussain, M. Suhail, S. D. Mukhtar, D. R. Sahoo, L. Asnin and I. Ali, *Chirality*, 2016, **28**(9), 642–648.
23 Y. Q. Yao, P. L. Song, X. L. Wen, M. D. Deng, J. Wang and X. J. Guo, *J. Sep. Sci.*, 2017, **40**, 2999–3007.

